The transformation suppressor gene *Reck* is required for postaxial patterning in mouse forelimbs

Mako Yamamoto[1,2], Tomoko Matsuzaki[1], Rei Takahashi[3], Eijiro Adachi[4], Yasuhiro Maeda[1], Sachiyo Yamaguchi[1,2], Hitoshi Kitayama[1], Michiko Echizenya[1], Yoko Morioka[1], David B. Alexander[5], Takeshi Yagi[6], Shigeyoshi Itohara[7], Takashi Nakamura[8], Haruhiko Akiyama[8] and Makoto Noda[1,*]

[1]Department of Molecular Oncology, [2]Global COE Program and [8]Department of Orthopaedic and Musculoskeletal Surgery, Kyoto University Graduate School of Medicine, Sakyo-ku, Kyoto 606-8501, Japan
[3]Department of Pharmacotherapeutics, Faculty of Pharmaceutical Sciences, Doshisha Women's College of Liberal Arts, Kodo, Kyotanabe, Kyoto 610-0395, Japan
[4]Department of Matrix Biology and Regenerative Medicine, Kitasato University Graduate School of Medical Science, 1-15-1 Kitasato, Minami-ku, Sagamihara, Kanagawa 252-0373, Japan
[5]Department of Molecular Toxicology, Nagoya City University Graduate School of Medical Sciences, 1 Kawasumi, Mizuho-cho, Mizuho-ku, Nagoya 467-8601, Japan
[6]KOKORO-biology group, Laboratories for Integrated Biology, Graduate School of Frontier Biosciences, Osaka University 1-3 Yamadaoka, Suita, Osaka 565-0871, Japan
[7]Laboratory for Behavioral Genetics, RIKEN Brain Science Institute, 2-1 Hirosawa, Wako, Saitama 351-0198, Japan
*Author for correspondence (mnoda@virus.kyoto-u.ac.jp)

Biology Open 1, 458–466
doi: 10.1242/bio.2012638

Summary

The membrane-anchored metalloproteinase-regulator RECK has been characterized as a tumor suppressor. Here we report that mice with reduced *Reck*-expression show limb abnormalities including right-dominant, forelimb-specific defects in postaxial skeletal elements. The forelimb buds of low-*Reck* mutants have an altered dorsal ectoderm with reduced *Wnt7a* and *Igf2* expression, and hypotrophy in two signaling centers (i.e., ZPA and AER) that are essential for limb outgrowth and patterning. *Reck* is abundantly expressed in the anterior mesenchyme in normal limb buds; mesenchyme-specific *Reck* inactivation recapitulates the low-*Reck* phenotype; and some teratogens downregulate *Reck* in mesenchymal cells. Our findings illustrate a role for Reck in the mesenchymal-epithelial interactions essential for mammalian development.

Key words: Mouse, Reck, Wnt7a, Limb patterning, Cutaneous horn, Teratogens

Introduction

Vertebrate limb patterning is controlled by two signaling centers, the zone of polarizing activity (ZPA) in the distal-posterior mesenchyme and the apical ectodermal ridge (AER) at the distal tip of the limb bud. The ZPA and AER produce signaling molecules (Shh and Fgfs, respectively) that control the formation of anterior-posterior and proximal-distal limb axes in a cooperative manner (Saunders, 1948; Johnson and Tabin, 1997; Tabin and Wolpert, 2007; Mariani et al., 2008; Towers and Tickle, 2009; Zeller et al., 2009). Another signaling molecule, Wnt7a, produced by the limb bud dorsal ectoderm (DE) controls the formation of the dorsal-ventral limb axis and activates Shh-expression in the ZPA, thereby influencing anterior-posterior limb patterning as well (Parr and McMahon, 1994; Riddle et al., 1995; Yang and Niswander, 1995).

RECK is a membrane-anchored glycoprotein of 125 kDa which forms dimers and regulates a wide variety of extracellular metalloproteinases, including several MMP family members (e.g., MMP7, 9, and 14), ADAM10, and CD13 (Takahashi et al., 1998; Oh et al., 2001; Miki et al., 2007; Muraguchi et al., 2007; Omura et al., 2009). RECK is down-regulated in various cancers (Noda and Takahashi, 2007), and restored RECK expression in cancer cells suppresses their malignant behavior (Takahashi et al., 1998; Oh et al., 2001), suggesting the potential importance of RECK as a prognostic indicator and therapeutic effector.

Reck-deficient mice die around embryonic day 10.5 (E10.5) with reduced tissue integrity and defects in vascular and neural development (Oh et al., 2001; Muraguchi et al., 2007; Chandana et al., 2010), suggesting its importance in relatively early events in mammalian development. The embryonic lethality of the conventional *Reck*-deficient mice, however, limits our understanding of its roles in the later stages of development and adult homeostasis. In this study, we employed hypomorphic and conditional *Reck* mutant mice to circumvent this limitation and found an essential role for *Reck* in forelimb development.

Materials and Methods

Mice

All the animal experiments were approved by the Animal Research Committee, Graduate School of Medicine, Kyoto University and conducted according to the guidelines of Kyoto University. The mouse carrying the R_{Low} allele (Acc. No. CDB0488K; http://www.cdb.riken.jp/arg/mutant%20mice%20list.html) was described elsewhere as an intermediate for obtaining the *R2* allele (Chandana et al., 2010). The founder mouse was back-crossed four times with C57BL/6 mice before intercrossing with mice heterozygous for the *Reck*-null (*R1Δ*) allele (Fig. 1A (3)) to yield R_{Low} / - (low-*Reck*) and R_{Low} / + (control) mice. To generate mice

carrying the *R1* allele (Fig. 1A (4)), a targeting vector (pRCKO-2, 13.85 kb) containing 6 components [from 5′ to 3′, (1) 3.9 kb 5′-arm, (2) loxP site, (3) 0.99 kb exon 1-containing fragment, (4) PGK-neo cassette franked by two loxP sites, (5) 1.9 kb 3′-arm, and (6) DT-A gene] was constructed using two vectors, loxP3-Neo and pMC1DTpA (Taniguchi et al., 1997), and a genomic DNA clone previously described (Sasahara et al., 1999). A mutant ES clone isolated after electroporation of linearized pRCKO-2 into E14 ES cells was used to produce a transgenic line following established protocols (Gomi et al., 1995), and the line was subsequently crossed with *EIIA-Cre* transgenic mice (Lakso et al., 1996) to eliminate the PGK-neo fragment alone or to eliminate the fragment together with exon 1 to obtain the alleles *R1* and *R1Δ*, respectively (supplementary material Fig. S1). The *R1* allele contains two loxP sequences at the Bms1 and HindIII sites that flank *Reck* exon 1, and the *R1Δ* allele lacks the sequence between the two loxP sequences. The founder mice were back-crossed six times with C57BL/6 mice before intercrossing with various Cre-driver mice. DNA from adult mouse tail or embryonic yolk sac was used for genotyping by PCR under the conditions described in supplementary material Table S5. The Cre reporter mouse *R26R* was a gift from P. Soriano (Soriano, 1999). The *Prx1-Cre* (Logan et al., 2002) and *Col2a1-Cre* (Ovchinnikov et al., 2000) transgenic mice were maintained and genotyped as previously described (Akiyama et al., 2002). The *Reck-CreER*^{T2} allele contains the CreER^{T2} coding sequence in-frame after codon 7 in *Reck* (T.M. et al., unpublished). In timed mating, the noon of the day of a vaginal plug was considered as E0.5.

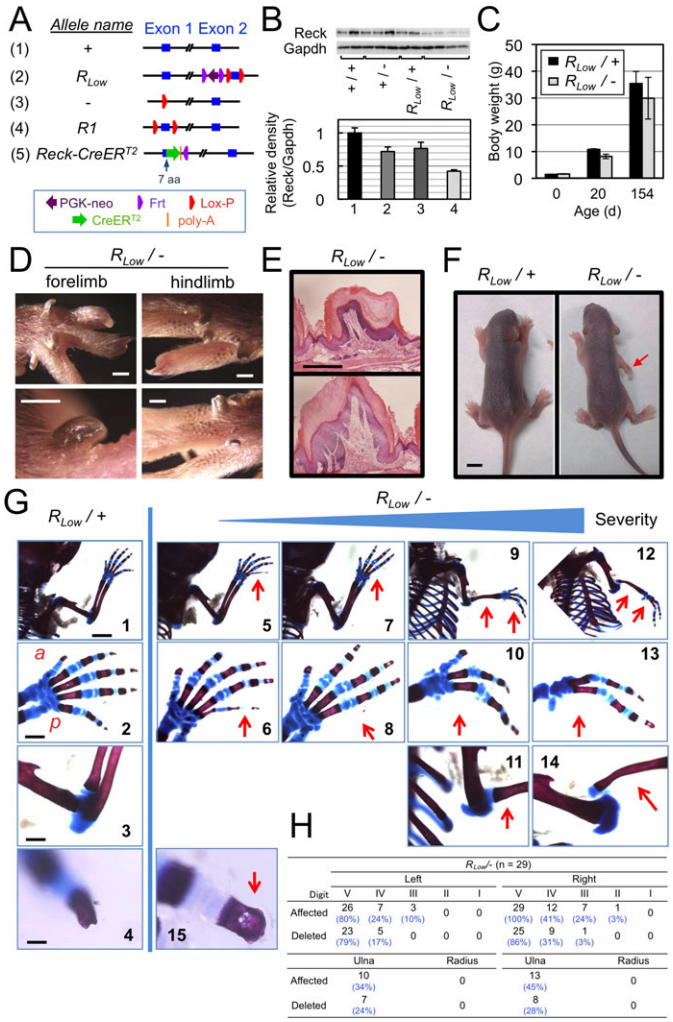

Fig. 1. Dermal and skeletal abnormalities found in low-*Reck* mutant mice. (**A**) Schematic representation of the 5′-terminal region of the five *Reck* alleles used in this study. (**B**) Immunoblot detection of Reck protein in whole E12.5 embryos. Each lane in the upper panels represents one embryo of the indicated genotype. Gapdh was used as a loading control. The lower bar graph summarizes the densitometry results (mean±SEM). (**C**) Body weights of control (R_{Low}/+; n=12) and low-*Reck* mutant (R_{Low}/-; n=6) mice at three time points after birth. (**D**) Gross morphology of typical cutaneous horns which developed on the dorsal surface of autopods in 4-week old R_{Low}/- mice. Scale bar, 1 mm. (**E**) Sections of cutaneous horn tissues stained with Haematoxylin and Eosin. Scale bar, 300 µm. (**F**) Dorsal views of a typical R_{Low}/+ (control) mouse and a R_{Low}/- (hypomorphic mutant) mouse at day 3 after birth. Scale bar, 5 mm. (**G**) Skeletal morphology of the right forelimbs (panels 1-3 and 5-14) and fingertips (panels 4 and 15) of neonatal mice. One control mouse (R_{Low}/+; panels 1–4) and four hypomorphic mutant mice with different degrees of severity (R_{Low}/-; panels 5–15) are compared. Scale bars: 2 mm in panels 1, 5, 7, 9, 12; 700 µm in panels 2, 3, 6, 8, 10, 11, 13, 14; 150 µm in panels 4, 15. The mutant sample shown in panels 12–14 has digit I, although this digit is unclear in these photographs. (**H**) The left-right asymmetry of the skeletal phenotype in R_{Low}/- mice. The number of animals (total 29) in which the indicated digits or zeugopod bones are affected (smaller and/or bent) or deleted was scored. No defects were found in the hindlimbs of these animals (data not shown). In contrast, cutaneous horns (D, E) and round porous fingertip bones (G, panel 15) are found in all extremities.

Morphological examinations

Skeletal samples were stained with Alcian Blue 8GX (Chroma-Gesellschaft, 1A288) and Alizarin Red S (Chroma-Gesellschaft, 1F583) as previously described (McLeod, 1980). For scanning electron microscopy, E11.5 embryos (n=4 for each genotype) were immersed in Zamboni's fixative for 12 h, and cut into two halves at the sagittal plane to identify right and left limb buds. The samples were post-osmificated, dehydrated, and immersed in t-butyl alcohol. They were then freeze-dried, coated with platinum, and examined using a scanning electron microscope (JSM 6360, JEOL, Tokyo, Japan). Ten images were recorded from each embryo. For histochemical analysis by light microscopy, tissue blocks were fixed in 4% PFA, embedded in paraffin, and sliced into 5 µm-thick sections which were subjected to hematoxylin and eosin (HE) staining following standard protocols. *In situ* TUNEL assay using ApopTag Plus Peroxidase *In Situ* Apoptosis Detection Kit (Chemicon, S7101) was performed as described previously (Smith and Cartwright, 1997). Whole-mount *in situ* hybridization (WISH) using digoxygenin-labeled RNA probes was performed as described previously (Conlon and Rossant, 1992; Parr and McMahon, 1994; Akiyama et al., 2002). To detect *Reck* mRNA, the 1092-bp Hind III-fragment from a mouse *Reck* cDNA (Accession, NM_016678; position, 1669–2760) was used to generate an antisense ribo-probe. At least 3 embryos per group were examined, and the features common to the majority of samples were recorded. Experiments were repeated at least twice to confirm reproducibility.

Analyses of proteins and RNAs

Immunoblot assays using antibodies against Reck (5B11D12), Gapdh (Ambion, AM4300), and α-tubulin (Calbiochem, CP06) were performed as described previously (Oh et al., 2001). Densitometry was performed using ImageJ software. For qRT-PCR, total RNA was isolated from mouse tissues or cell lines (1×10^6 cells/60-mm dish) using NucleoSpin RNA II (Macherey-Nagel, 740955) and subjected to qRT–PCR as described previously (Hatta et al., 2009) with additional primers newly designed for *Wnt7a* and *Igf2* (supplementary material Table S5).

Cell culture

ATDC5 cells and their transfectants have been described previously (Atsumi et al., 1990; Shukunami et al., 1996; Kondo et al., 2007). MKE cells derived from newborn mouse kidney were maintained in chemically defined medium (T.M. et al., unpublished). Sources of cytokines and teratogens used to study their effects on gene expression in these cells: Shh (R & D Systems, 464-SH), Wnt7a (R & D Systems, 3008-WN), Fgf8 (R & D Systems, 423-F8), Igf2 (R & D Systems, 792-MG), $CdCl_2$ (nacalai tesque, 06613), acetazolamide (Sigma, A6011), thalidomide (Sigma, T144), and ethanol (nacalai tesque, 14713).

Fate mapping

R26R/R26R female mice were crossed with male mice carrying one *Reck-CreER*^{T2} allele, and 2 mg tamoxifen (TMX; Sigma, T5648; 20 mg/ml-corn oil) was injected intraperitoneally into the pregnant mice at a time point between post-coital day 7.5 and 11.5. The embryos were harvested at a time point between E10.5 and E12.5 and subjected to X-gal staining as described previously (Ahn and Joyner, 2004). To investigate the fates of *Reck*-expressing cells in the mutant mice, R_{Low}/R_{Low} female mice were mated with male mice with the genotype *Reck-CreER*^{T2}*/+;R26R/R26R*, and the pregnant mice were treated with TMX. Offspring with the genotype of R_{Low}*/ Reck-CreER*^{T2}*;R26R/+* were analyzed.

Transcriptome analyses

ATDC5 cells stably transfected with a control vector (LXSN) or the vector expressing human *RECK* (Kondo et al., 2007) were plated at 6.5×10^5 cells per 100-mm dish and cultured for 3 days. Total RNA extracted using RNeasy Kit

(QIAGEN) was subjected to gene expression profiling using the Mouse Genome 430 2.0 Array (Affymetrix, Santa Clara, CA). To analyze the gene expression profile *in vivo*, total RNA was extracted from pooled right forelimb buds excised from E12.5 embryos (n≥11). Data were adopted only when one or both of the data being compared showed positive flag(s). Up-regulation was defined by a ratio greater than 2 and down-regulation by a ratio smaller than 0.5. The online program FunNet (Prifti et al., 2008) was used to find the pathways (KEGG) and biological processes (GO) significantly affected.

Results

Hypomorphic *Reck* mutant mice show limb abnormalities

To understand the roles of *Reck* in late-stage development (after E10.5) and adult homeostasis, we established several lines of *Reck* mutant mice (Fig. 1A). One of the intermediate products, which retains the selection marker PGK-neo in front of exon 2 (Fig. 1A (2)) (Chandana et al., 2010), was found to express Reck protein at less than one half the level of the wild type allele (Fig. 1B bar 4); we therefore call this allele R_{Low} and animals hemizygous for this allele (R_{Low}/-) low-*Reck* mutants. Low-*Reck* mutants and their heterozygous littermates (R_{Low}/+; control) are comparable in their body weights (Fig. 1C). The low-*Reck* mutants, however, have remarkable limb abnormalities; they have multiple cutaneous horns on the dorsal side of their extremities (Fig. 1D,E) and, in some cases, one or both of their forelimbs are pointing backwards (Fig. 1F red arrow). Skeletal preparations of newborn low-*Reck* mutants show loss of postaxial forelimb structures with variable severity (Fig. 1G); forelimbs pointing backwards represent the absence of ulna (Fig. 1G panels 11 and 14). The skeletal phenotype tends to be more severe in the right forelimb (Fig. 1H). In contrast, the cutaneous horns occur in all limbs, albeit in varying severity, with almost 100% penetrance; the lesions in the forelimbs tend to be longer and pointed as compared to the lesions in the hindlimbs. In addition, fingertip bones are round and porous in all limbs of low-*Reck* mutants (Fig. 1G panel 15).

Reduced Reck expression affects some early events in forelimb development

Abnormal morphology of the forelimb buds of low-*Reck* mutants is evident as early as E12.5: the posterior side is hypoplastic (Fig. 2A panel 2 red arrow) and shows poor chondrocyte condensation (blue signals). Slices of mutant limb buds show altered cytoarchitecture, e.g., increased cell density in the central area and uneven, spongy distribution of cells in the marginal areas (Fig. 2B panel 2). Increased apoptosis, however, was not detectable around the hypoplastic area (Fig. 2C arrow). Forelimb bud hypoplasia can also be observed in scanning electron micrographs (SEM), especially in the posterior region of the mutant's forelimbs (Fig. 2D panels 2 and 4 arrow). Interestingly, the AER, which is robust in the control samples (Fig. 2D panels 5 and 7 bracket), is flattened in the low-*Reck* mutants (Fig. 2D panels 6 and 8 arrows). Also, the DE cells in the mutant limb buds have a distinctly altered appearance (Fig. 2D panel 10). Finally, the underlying mesenchymal cells and the ECM appear to have decreased integrity compared to those underlying the DE of the control limb buds (Fig. 2D panels 12 and 11; supplementary material Fig. S2).

Our previous study implicated *Reck* in chondrocyte differentiation *in vitro* (Kondo et al., 2007). To test whether reduced *Reck* expression in developing cartilage is responsible for the skeletal phenotype of low-*Reck* mice, we generated mutant mice (*R1/-;Col2a1-Cre*) in which *Reck* is inactivated selectively in the late-stage mesenchymal cells committed to the chondrocyte lineage. These mice, however, show no obvious defects in limb patterning (supplementary material Fig. S3).

We also generated another mutant line (*R1/-;Prx1-Cre*) in which *Reck* is inactivated in undifferentiated limb mesenchyme; these mice show skeletal defects (Fig. 2E) reminiscent of those in R_{Low}/- mice (Fig. 1G). Hence, Reck in undifferentiated limb mesenchyme seems to be critical for proper forelimb development.

Fates of *Reck*-positive cells in normal limb buds

How can we explain the abnormal cytoarchitecture found in the mutant forelimb buds (Fig. 2B)? To address this issue, we analyzed the fates of *Reck*-positive cells in mice carrying a *Reck-CreER^{T2}* allele (Fig. 1A (5)) and the *ROSA26* reporter system (Soriano, 1999). Although the resulting mice (i.e., +/ *Reck-CreER^{T2};R26R*) are normal in phenotype, the cells expressing *Reck* can be tagged by injecting tamoxifen (TMX) into the animal and staining with X-gal. In our first set of experiments, we injected TMX into pregnant mice at different time points and stained the embryos at E12.5 (Fig. 3A). Interestingly, the proximo-anterior regions of four limbs are among the most prominent areas of staining under these conditions. We also found that labeled cells were most abundant and widely distributed when TMX was injected at E8.5 (Fig. 3A panels 3 and 4); interestingly, the signals tended to be stronger in the hind- and left limbs (for expanded views, see supplementary material Fig. S4).

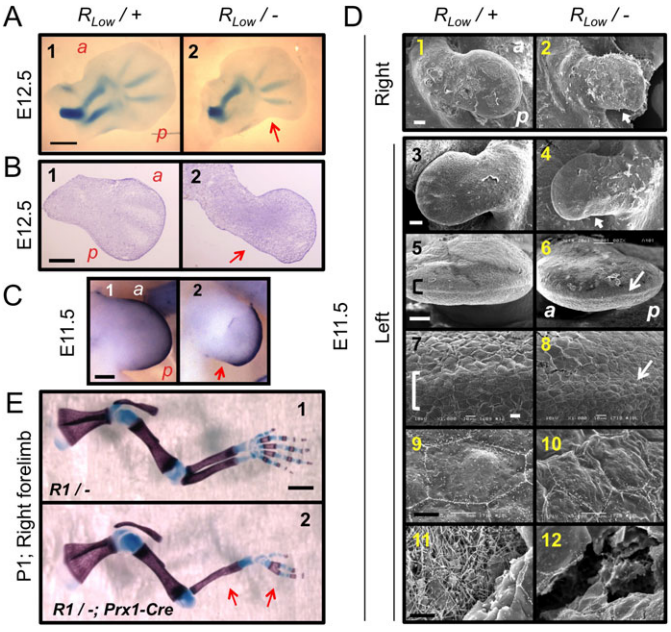

Fig. 2. Morphology of forelimbs in hypomorphic or conditional *Reck* mutant mice. (**A-D**) R_{Low}/+ (left panels) and R_{Low}/- (right panels) littermates were harvested at the indicated stages and analyzed by whole-mount Alcian Blue-staining (A), HE-staining of limb sections (B), whole-mount *in situ* TUNEL assay (C), and SEM (D). Arrows indicate hypoplasia. Bracket in D indicates robust AER. Scale bar: 200 μm in A and B; 100 μm in C and D panels 1–6; 10 μm in D panels 7, 8; 5 μm in D panels 9-12. Orientation: *a*, anterior; *p*, posterior. (**E**) Effects of selective *Reck* inactivation in early limb mesenchyme. Skeletal preparations of neonatal *R1/-* (Cre-negative control) and *R1/-;Prx1-Cre* mice are compared. Arrows indicate postaxial skeletal defects reminiscent of those in R_{Low}/- mice. Scale bar, 500 μm.

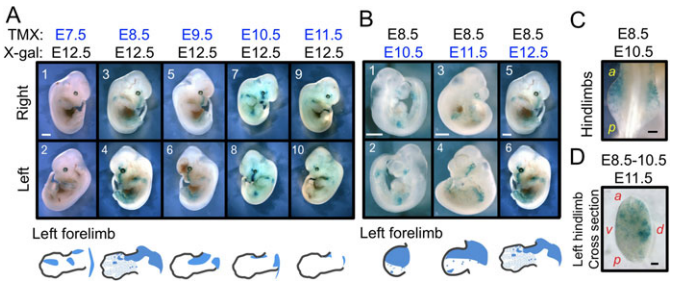

Fig. 3. Distribution and fates of *Reck*-positive cells in normal embryos. (**A**) Distribution of *Reck*-positive cells in embryos treated at four different time points (E7.5 - E11.5) and visualized at a fixed time point (E12.5). The right (top row) and left (second row) views of the same embryo are shown. The bottom cartoon illustrates the distribution of signals in the left forelimb, which generally shows more abundant signals than the right forelimb. (**B**) Distribution of *Reck*-positive cells tagged at a fixed time point (E8.5) and visualized at three different time points (E10.5 - E12.5). The same sample is shown in A (panels 3 and 4) and B (panels 5 and 6) for comparison. (**C**) Dorsal view of the hindlimb region of an embryo treated with tamoxifen at E8.5 and stained with X-gal at E10.5. (**D**) Cross section of the left hindlimb of an embryo treated with tamoxifen 3 times (E8.5, E9.5, and E10.5) and stained with X-gal at E11.5. Scale bar: 1 mm in A, B; 200 μm in C; 100 μm in D. Orientation: *a*, anterior; *p*, posterior; *d*, dorsal; *v*, ventral.

In our second set of experiments, we injected TMX at E8.5 and stained the embryos at different time points (Fig. 3B). At E10.5, the *Reck*-positive cells were most abundant in the proximo-anterior region, forming a gradient toward the distal-posteior margin (Fig. 3B panels 1 and 2). At the later time points, the labeled cells were increased in number and distributed more widely along the anterior edge of the limb bud (Fig. 3B panels 3–6). In the dorsal view (Fig. 3C) and in cross sections of limb buds (Fig. 3D), signals are predominantly found in the mesenchymal tissue. Taken together, these findings suggest that the *Reck*-positive mesenchymal cells present in the proximo-anterior region of the limb buds at around E9 proliferate and spread toward the distal end.

Fates of *Reck*-positive cells in the mutant limb buds

Next, to ask whether *Reck* hypomorphism has any effect on mesenchymal cell behavior, we took advantage of the *Reck-CreER*^{T2} allele which is null in terms of *Reck* gene function (Fig. 1A (5)). Namely, R_{Low}/*Reck-CreER*^{T2};*R26R* mice (labeled R_{Low} in Fig. 4) are low-*Reck* mutants which can be used to trace the fate of *Reck*-positive cells (detected as LacZ$^+$ cells). When these mice were treated with TMX at E8.5 and stained at E10.5, LacZ$^+$ cells were fewer and located more centrally in the limb bud (Fig. 4A panels 3 and 4) as compared to the control (+/*Reck-CreER*^{T2};*R26R*) (Fig. 4A panels 1 and 2). One day later (i.e., embryos stained at E11.5), the number of LacZ$^+$ cells increased, but their distribution was abnormal in the mutants: compared to the control, small clusters of LacZ$^+$ cells were scattered more widely and to the posterior side, and the signals tended to be less dense in the distalo-anterior region (Fig. 4B panels 5–8). Hence, *Reck* hypomorphism has a significant impact on the spatial distribution of *Reck*-positive cells.

Signaling from the DE, ZPA, and AER is attenuated in the low-*RECK* mutant limb buds

To obtain more information regarding the mechanism of low-*Reck* limb abnormalities, we examined the expression of several genes involved in limb patterning in the mutant (R_{Low}/-) and control (R_{Low}/+) mouse embryos by whole-mount *in situ* hybridization (WISH). Known functional intereactions among the products of these genes during limb development are summarized in supplementary material Fig. S5 (Parr and McMahon, 1994; Riddle et al., 1995; Yang and Niswander, 1995; Johnson and Tabin, 1997; Niswander, 2003; McGlinn and Tabin, 2006; Tickle, 2006; Zeller et al., 2009). We found that the *Lmx1b*-postive compartment was smaller and the *En1*-positive area expanded and mis-located in the mutant forelimb buds (Fig. 5A panels 2, 4 and 6; supplementary material Fig. S6A panels 2 and 4). Of note, a similar phenotype has been found in mice with reduced Wnt7a-signaling (Adamska et al., 2005).

At E10.5, *Shh* expression is detectable but somewhat weaker than the control in the mutant right forelimb buds (Fig. 5B panel 2; supplementary material Fig. S6A panels 5 and 6). At E11.5, the area normally positive for *Shh* (i.e., the ZPA) is partially missing in the mutants (Fig. 5C panel 2). In addition, direct targets of *Shh*-signaling, e.g., *Ptch1* and *Gli1,* are also downregulated in mutant samples (Fig. 5B panel 10, Fig. 5C panel 4). Signals of another Shh target, *Grem1*, are decreased at E10.5 in mutant right forelimbs (Fig. 5B panel 6); at E11.5 the Grem1 signals are more aggregated in the central region than those in the control samples (Fig. 5C panel 6 vs. panel 5).

Two *Fgf* family genes (*Fgf8* and *Fgf4*) expressed in the AER are downregulated in mutant samples at E10.5 (Fig. 5B panels 8 and 12); at E11.5, the AER (marked by *Fgf8*) is often truncated on both termini (anterior and posterior) and sometimes discontinuous near the posterior end (Fig. 5C panel 8; supplementary material Fig. S6B panels 3 and 4). Again, a similar AER truncation has been found in mice with reduced Wnt7a-signaling (Adamska et al., 2004). Hence, although these

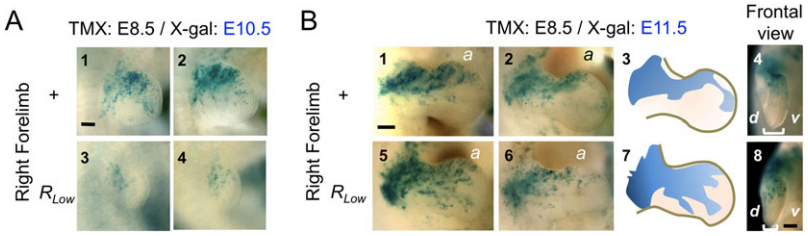

Fig. 4. Effects of low-*Reck* mutation on the distribution of *Reck*-positive cells. (**A**) Distribution of *Reck*-positive cells tagged at E8.5 and visualized at E10.5. Right forelimbs of two typical control (+/*Reck-CreER*^{T2};*R26R*) (panels 1, 2) and mutant (R_{Low}/*Reck-CreER*^{T2};*R26R*) (panels 3, 4) embryos are shown. (**B**) Distribution of *Reck*-positive cells tagged at E8.5 and visualized at E11.5. Right forelimbs of two typical control (panels 1, 2) and mutant (panels 5, 6) embryos, together with schematic representations of the results (panels 3, 7), are shown. Frontal views of the right forelimbs of one control and one mutant embryo are shown (panels 4, 8). Bracket denotes the thickness of the limb bud. Scale bar, 200 μm.

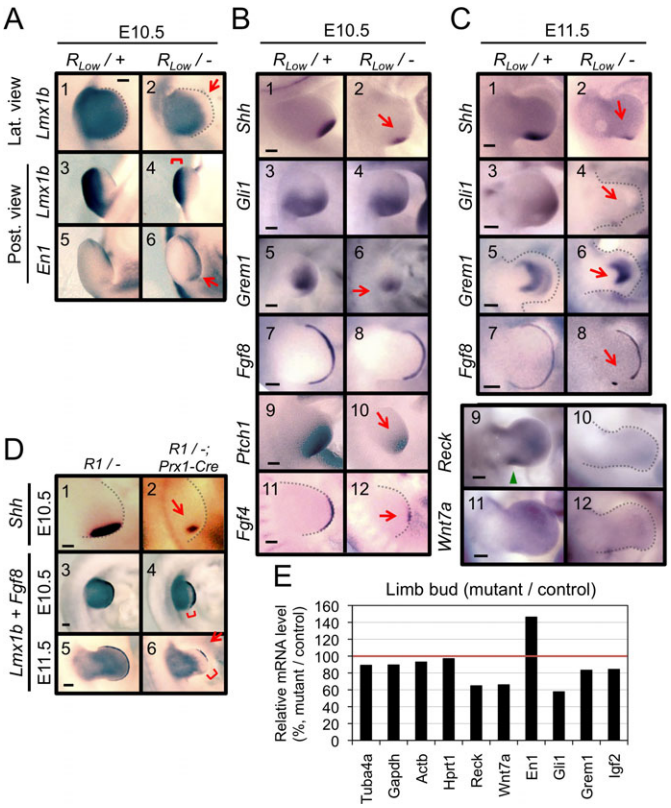

Fig. 5. Effects of low-*Reck* mutation on the expression of morphogenetic signaling molecules and their targets. (**A**) Effects of low-*Reck* mutation on Wnt7a-signaling. Expression of positive (*Lmx1b*) and negative (*En1*) targets of Wnt7a-signaling in right forelimb buds were visualized by WISH. Lateral (Lat.) and posterior (Post.) views of right forelimb buds are shown. Note the widened *Lmx1b*-negative margin (panel 2, arrow), narrowed *Lmx1b*-positive area (panel 4, bracket), and expanded *En1*-positive area (panel 6, arrow) in R_{Low}/- right forelimb buds. (**B**,**C**) Effects of low-*Reck* mutation on direct or indirect targets of Shh-signaling. Expression of the indicated genes in the right forelimbs of R_{Low}/+ or R_{Low}/- littermates harvested at E10.5 (B) or E11.5 (C) were visualized by WISH. Red arrows indicate reduced (or abnormally distributed) hybridization signals. Green arrowhead in C panel 9 indicates posterior *Reck* signal. (**D**) Effects of selective *Reck*-inactivation in early limb mesenchyme on morphogenetic signals. The expression of *Shh*, *Lmx1b*, and *Fgf8* in the forelimb buds of control (*R1/-*) or conditional (*R1/-;Prx1-Cre*) mutant littermates were visualized by WISH. Note the reduced *Shh*-positive area (panel 2, arrow), widened *Lmx1b*-negative margin (panels 4 and 6, bracket), and reduced *Fgf8*-positive areas in the conditional mutant mice (panel 6, arrow). Scale bar in A-D, 200 µm. (**E**) Effects of low-*Reck* mutation on gene expression in the right forelimb buds. Total RNA extracted from the right forelimb buds of R_{Low}/+ (control) or R_{Low}/- (mutant) mice at E12.5 (n=11) was subjected to gene expression profiling. In cases where multiple probes for a single gene were included in the microarray, the value for the most abundant species is shown.

WISH data suggest attenuated signaling from all three morphogenetic centers (i.e., DE, ZPA, and AER), the low-*Reck* mutant shares many aspects in common with *Wnt7a*-deficient mice in their embryonic limb phenotypes.

We also analyzed the gene expression profiles of right forelimbs from the mutant and control embryos at E12.5 and found down-regulation of *Reck*, *Wnt7a*, and *Gli1* as well as up-regulation of *En1* in the mutant (Fig. 5E), supporting the WISH data.

As described above, selective knockout of *Reck* in early mesenchyme (*R1/-;Prx1-Cre* mice) caused skeletal defects similar to those of the low-*Reck* mutants. Importantly, reduced expression of *Shh*, *Lmx1b*, and *Fgf8* was also detected in these mice (Fig. 5D), further supporting the idea that reduced *Reck* expression in the early limb mesenchyme is responsible for the postaxial defects found in the forelimbs of low-*Reck* mutants.

Distribution of *Reck* and *Wnt7a* mRNA in E11.5 right forelimb buds

To verify the *Reck* distribution visualized in the fate-mapping study, we tried to directly detect *Reck* mRNA in E11.5 embryos by WISH (Fig. 5C panels 9 and 10), using a newly designed probe. In the control embryos, the *Reck*-positive areas overlapped with, but were somewhat larger than, the areas detected with the *Reck-CreER^{T2};R26R* system (compare Fig. 5C panel 9 to Fig. 4B panels 1 and 2). As expected, *Reck* signals were weaker in low-*Reck* embryos than in the control embryos (Fig. 5C panels 10 and 9), particularly in their right forelimbs (supplementary material Fig. S6C panel 4).

We also tried to visualize *Wnt7a* mRNA by WISH (Fig. 5C panels 11 and 12). Of note, there was considerable overlap between the areas of abundant *Wnt7a* signals and the *Reck*-positive areas in the forelimb buds in control animals, especially in their anterior region (compare Fig. 5C panel 9 and panel 11; supplementary material Fig. S7A). Importantly, *Wnt7a* signals were consistently lower in the mutant forelimb buds as compared to the control samples (Fig. 5C panels 12 and 11), especially in their right forelimbs (supplementary material Fig. S6D panel 4). These findings support the idea that Reck is required for the maintenance of Wnt7a production in the limb tissue.

Does Reck expressed in the limb mesenchyme play any inductive role in limb patterning? To test this model, we tried to ectopically express *Reck* in early limb mesenchyme (supplementary material Fig. S8A). A mouse expressing the *Reck* transgene in a posterior domain of its forelimb, however, showed no obvious abnormality in limb patterning (supplementary material Fig. S8B panel 2), suggesting that the action of *Reck* in this system may be supportive rather than inductive.

Gene expression *in vitro*

To better understand how Reck works in the limb tissues, we analyzed the effects of *RECK* over-expression on the gene expression profile of a chondrogenic cell line, ATDC5, which shares many properties with undifferentiated mesenchyme (Atsumi et al., 1990; Shukunami et al., 1996). *RECK* up-regulates genes involved in cell adhesion and the cell cycle while it down-regulates genes involved in pathways in cancer, focal adhesion, MAP-kinase signaling, regulation of the actin cytoskeleton, and chemokine signaling (supplementary material Tables S1 and S2; summarized in Fig. 6A). In addition, prominent induction of *Igf2* (supplementary material Table S3) and down-regulation of several genes involved in cytokine/chemokine signaling (supplementary material Table S4) were also detected. On the other hand, *Wnt7a* mRNA was undetectable even after *RECK* expression in this mesenchymal cell line (data not shown), making it less likely that Reck induces Wnt7a-expression directly in the limb mesenchyme.

Igf2 is an insulin-related growth factor essential for normal fetal growth and development (DeChiara et al., 1990). Indeed, *Igf2* mRNA is abundant in the right forelimb tissues from the control embryos at E12.5 but less abundant in the samples collected from low-*Reck* mice (Fig. 6C bottom panel bars 3 and

4). To test the simple model that Igf2 (probably produced by mesenchymal cells) promotes *Wnt7a*-expression in epithelial cells, we used a mouse epithelial cell line, MKE, that does not express *Igf2*. We found, however, that no significant changes in the level of *Wnt7a* mRNA were detectable after Igf2-treatment of MKE cells (Fig. 6B bar 2). Instead, we found that treatment with exogenous WNT7A resulted in a dramatic down-regulation of endogenous *Wnt7a* mRNA (Fig. 6B bar 3), demonstrating tight, negative feedback regulation of *Wnt7a* expression in these cells.

We also analyzed the effects of several signaling molecules on Reck-expression in ATDC5 cells (Fig. 6D). Since our previous study with fibroblasts indicated that the level of Reck-expression is under the strong influence of cell density (Hatta et al., 2009), we treated the cells at two different cell densities. Reck was upregulated by WNT7A, Fgf8, and Igf2 (Fig. 6D bars 6, 8 and 10) but not by Shh (Fig. 6D bar 4).

Effects of teratogens on Reck-expression

Several teratogens induce right-dominant, postaxial ectrodactyly in mouse forelimbs (i.e., an almost perfect phenocopy of the R_{Low}/- mutant) when the animals are exposed to these agents around E9.5 (Bell et al., 2005; Schreiner et al., 2009). Interestingly, some of the teratogens, e.g., cadmium and ethanol, down-regulate endogenous Reck in ATDC5 cells (Fig. 6E), implicating RECK as a target of these teratogens.

A

Biological processes or pathways affected by RECK in ATDC5 cells

Up-regulated* [GO Biological Processes]	Down-regulated* [KEGG Pathways]
Cell adhesion (14)	Pathways in cancer (15)
Cell cycle (12)	Focal adhesion (9)
Nervous system development (6)	MAPK signaling pathway (9)
Heart development (5)	Regulation of actin cytoskeleton (8)
Glycolysis (4)	Chemokine signaling pathway (7)
tRNA aminoacylation for protein translation (3)	Leukocyte transendothelial migration (5)
Protein amino acid autophosphorylation (3)	Arrhythmogenic right ventricular cardiomyopathy (4)
Fatty acid biosynthetic process (3)	Citrate cycle (3)
	Riboflavin metabolism (3)

( ) number of genes

*Total number of genes affected: up-regulated 185, down-regulated 101

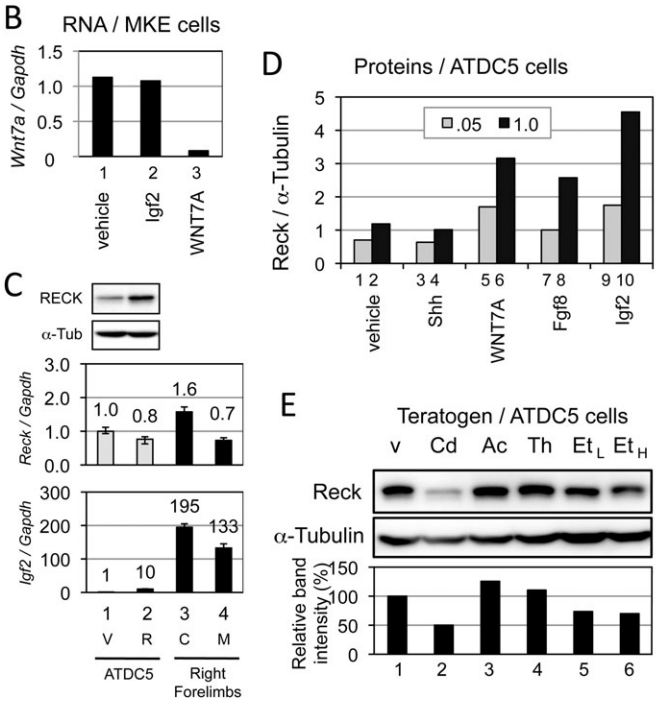

Fig. 6. Effects of RECK, morphogenetic cytokines, and teratogens detected in cultured cells. (**A**) Effects of *RECK*-expression on gene expression in ATDC5 cells. Total RNA extracted from ATDC5 cells stably transfected with a control retroviral vector or the vector expressing *RECK* was subjected to gene expression profiling. GO-biological processes and KEGG-pathways substantially affected by *RECK*-expression are listed with the number of genes involved (see supplementary material Tables S1–S4 for genes and Affymetrix IDs). (**B**) Effects of Igf2 and WNT7A on endogenous *Wnt7a* expression in epithelial cells. MKE cells (1×10^6 cells per 60-mm dish) plated on the previous day were treated for 24 h with Igf2 (150 ng/ml) or WNT7A (200 ng/ml), and the total RNA was subjected to qRT-PCR to determine the levels of *Wnt7a* and *Gapdh* (loading control) mRNAs. (**C**) *Reck* and *Igf2* mRNAs determined by qRT-PCR. Total RNA from the ATDC5 transfectants used in A (bar 1, vector; bar 2, RECK) or from embryonic right forelimb tissues used in Fig. 5E (bar 3, R_{Low}/+; bar 4, R_{Low}/-) was subjected to qRT-PCR using primer sets for *Reck* (upper bar graph) or *Igf2* (lower bar graph) and *Gapdh* (internal standard). Overexpression of human RECK protein in the transfectants was confirmed by immunoblot assay (top panel); α-tubulin was used as an internal standard (second panel). The values relative to that of the vector-transfected ATDC5 cells (bar 1) are presented in both numbers and bar graphs. Note that this *Reck* primer set is specific to the mouse *Reck* mRNA. Abbreviations: V, vector; R, *RECK*; C, control (R_{Low}/+), M, mutant (R_{Low}/-). (**D**) Effects of morphogens and cytokines on Reck expression in ATDC5 cells. ATDC5 cells plated at two different cell densities, 5×10^4 per 35-mm dish (.05, grey bars) and 1×10^6 per 35-mm dish (1.0, black bars), on the previous day were treated for 24 h with either vehicle, Shh (1 μg/ml), WNT7A (200 ng/ml), Fgf8 (25 ng/ml), or Igf2 (150 ng/ml), and the lysates were subjected to immunoblot assay to estimate the levels of Reck and α-tubulin (loading control). (**E**) Effects of teratogens on Reck expression in ATDC5 cells. Cells plated at 3×10^5 cells per dish on the previous day were treated for 6 h with vehicle (v), 10 μM $CdCl_2$ (Cd), 1 mM acetazolamide (Ac), 1 mM thalidomide (Th), 7.25 mM ethanol (Et_L), or 500 mM ethanol (Et_H), and the cell lysates were subjected to immunoblot assay to estimate the levels of Reck and α-tubulin (loading control). The densitometric data for Reck (normalized against α-tubulin and divided by the value for vehicle) are shown in the bottom bar graph.

Discussion

For elucidating the physiological functions of Reck, conventional *Reck*-knockout mice have been of limited use, since they show embryonic lethality around E10.5 and provide little information on the functions of Reck in late-stage development and in the adult. One way to circumvent this obstacle would be to use mice with reduced *Reck* expression. The phenotypes of such animals may reveal biological processes heavily dependent on RECK. In the case of low-*Reck* mutants, the most obvious phenotype appears in their extremities (Fig. 1), and this is consistent with our finding that in mid-gestation embryos, limb buds are among the regions where *Reck*-positive cell are particularly abundant (Fig. 3). The limb phenotype may also reflect the lack of redundancy or the vulnerability in molecular circuitry regulating some critical step in limb development. We therefore decided to characterize these *Reck* hypomorphic mutant mice in detail, hoping to obtain fresh insight into the functions of Reck *in vivo*.

Morphological features found in the right forelimb buds of low-*Reck* mutants include (i) aberrant surface epithelium, (ii) hypoplastic distal-posterior margin, and (iii) a less well developed AER which is often discontinuous in its posterior region (Fig. 2D, Fig. 5C panel 8). These and other data (e.g., Fig. 5; see below) suggest that the *Reck* hypomorphic mice have defects in both the structure and function of three signaling centers, DE (producing Wnt7a), ZPA (producing Shh), and AER (producing Fgfs), essential for limb growth and patterning. Limb pattern abnormalities reminiscent of those in low-*Reck* mice have

been found in at least three systems: (i) mice with *Wnt7a*-deficiency either alone (Parr and McMahon, 1994) or in combination with *Lrp6*$^{+/-}$ mutation (Adamska et al., 2005), (ii) mice overexpressing a Wnt-signaling antagonist, SOST (Collette et al., 2010), and (iii) mice treated with certain teratogens (see below). On the other hand, mutations in the other signaling molecules or transcription factors involved in limb patterning, such as Shh (Chiang et al., 1996; Zhu et al., 2008), Lmx1b (Chen et al., 1998), En1 (Wurst et al., 1994), Grem1 (Michos et al., 2004), Bmp4 (Selever et al., 2004), and Fgf4/8 (Mariani et al., 2008), yield phenotypes distinct from those of low-*Reck* mice. Genetic evidence therefore suggests that deficiency in Wnt7a signaling is likely to be the immediate consequence of *Reck*-hypomorphism.

Our data in cultured cells (Fig. 6B) suggest the presence of an intrinsic negative feedback regulation that would allow homeostatic expression of Wnt7a from epithelial cells (Fig. 7C). In such a system, substantial reduction in Wnt7a expression (Fig. 5C panel 12, Fig. 5E; supplementary material Fig. S6D) is likely to result from a loss or malfunctioning of its source (i.e., limb bud DE). In the chicken system, removal of wing bud DE leads to the loss of Shh expression in the ZPA and the eventual loss of posterior components of the wing (Yang and Niswander, 1995), highlighting the importance of an intact DE for posterior morphogenesis in the limb. The aberrant DE in R_{Low}/- limb buds (Fig. 2D; supplementary material Fig. S2) suggest that *Reck* is important for the health of limb bud DE and hence, for a continuous supply of Wnt7a.

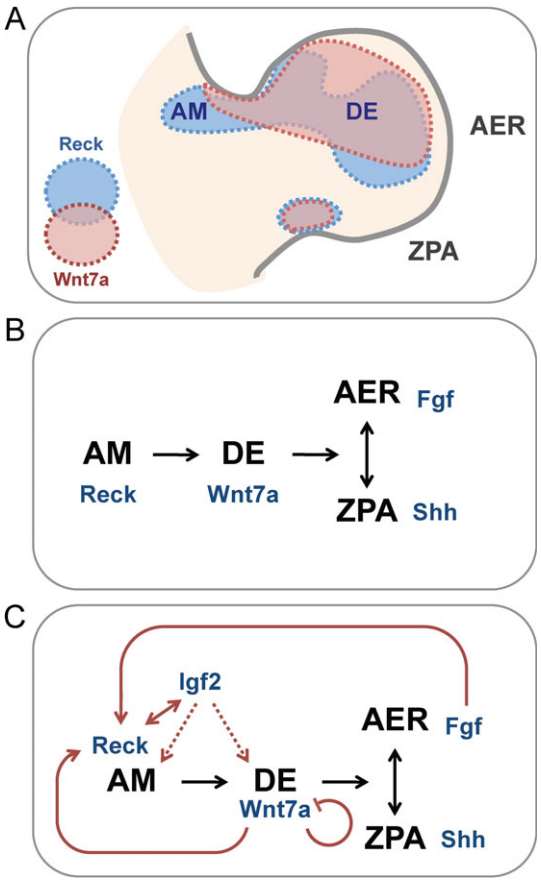

Fig. 7. Models consistent with our findings. (**A**) Distributions of *Reck* (Fig. 5C panel 9) and *Wnt7a* (Fig. 5C panel 11) mRNA in E11.5 forelimb bud. AM: anterior mesenchyme, DE: dorsal ectoderm. (**B**) Possible interactions between the tissues (black letters) and mediators (blue letters) of these interactions. (**C**) Feedback regulations (brown lines) among the tissues and mediators implicated in this study.

Several lines of evidence indicate that *Reck* expressed in the mesenchyme, rather than DE, is critical for forelimb development. First, *Reck* expression is detectable in cultured mesenchymal cells (Fig. 6C,D) but not in epithelial cells (transcriptome data, not shown). Second, in our fate-mapping studies, most *Reck*-reporter signals are found in the mesenchyme (Fig. 3C,D). Third and most importantly, selective inactivation of *Reck* in early mesenchyme (using the *Prx1-Cre* system) was sufficient to induce postaxial limb abnormalities (Fig. 2E). These findings imply a non-cell-autonomous nature for Reck activity in this system.

How do the *Reck*-positive mesenchymal cells support the health of DE? Our fate-mapping studies indicate that *Reck*-positive cells are abundant in the anterior meshenchyme (AM) in the limb bud of mid-gestation embryos (Fig. 3). Previous studies *in vitro* demonstrated that Reck is critical for stable cell-substrate adhesion and, slow but persistent, directional migration of fibroblasts (Morioka et al., 2009). Some features of mutant limbs, such as distalo-posterior (i.e., ZPA) hypotrophy (Fig. 2), altered cytoarchitecture (Fig. 2B panel 2), flattened AER (Fig. 2D panels 6 and 8), and abnormal distribution of *Reck*-positive cells (Fig. 4) may well be explained by the failure of the cells to migrate properly under reduced Reck expression. It is, however, unclear whether the apparent mis-behavior and abnormal distribution of the cells are causative to the limb defects found in low-*Reck* mice. In fact, several lines of evidence seem to go against this possibility. First, in the fate mapping study, very few *Reck*-positive cells were found near the distalo-posterior domain in the wild type embryos at E11.5 (Fig. 4B panels 1–4); by this time, tissue hypotrophy is already evident in low-*Reck* mutants. Second, the posterior *Reck*-positive domain detected by WISH (see below) does not coincide with the *Shh*-positive region (i.e., ZPA; supplementary material Fig. S7B). Third, as alluded to above, the eventual limb phenotype of low-*Reck* mice is quite distinct from that of *Shh*-deficient mice [loss of many skeletal elements, resulting in the limb consisting of a stylopod, a single reduced zeugopod element, and a single reduced digit (Chiang et al., 2001; Kraus et al., 2001)] or a series of *Fgf*-deficient mice [loss of antero-distal elements to complete failure of limb formation (Sun et al., 2002; Mariani et al., 2008)]. We therefore speculate that ZPA hypotrophy and AER flattening may not represent the immediate consequence of *Reck*-hypomorphism.

In contrast, the *Wnt7a*-positive areas and *Reck*-positive areas largely overlap in the dorsal views of the control limb buds (Fig. 5C panels 9 and 11; supplementary material Fig. S7A), and the level of *Wnt7a* mRNA is greatly reduced in the mutant right forelimb buds (Fig. 5C panel 12; supplementary material Fig. S6D). These data, together with the genetic, morphological, and biochemical evidence discussed above, support a model that Reck expression in the underlying mesenchyme helps maintain the health of the DE and its production of Wnt7a, thus promoting subsequent tissue interactions required for the establishment of a robust AER and ZPA (Fig. 7A,B).

A previous study on the developing central nervous system in the mouse revealed a role for Reck in suppressing neuronal

differentiation and expanding the neural precursor pool (Muraguchi et al., 2007). This mode of action fits with our findings that the mutant limb buds show hypotrophy without apoptosis (Fig. 2) and that fewer cells were labeled in the mutant limb buds in the fate-mapping studies (Fig. 4).

Unlike the fate-mapping data (Fig. 3), our WISH data showed strong *Reck* signals on the posterior side (Fig. 5C panel 9 green arrowhead; compare this panel with Fig. 4B panels 1 and 2), in addition to the AM. Whether this represents aberrant cross-reaction in hybridization probe, incomplete fidelity of *Reck-CreER*^{T2} expression, post-transcriptional regulation, or is due to some other reason needs to be clarified in future studies. Nevertheless, the expression of Reck in the AM is consistent between the two techniques.

What would be the mediator(s) of the tissue interactions discussed above? Our transcriptome data indicate that Reck can alter the levels of a cohort of mRNAs in mesenchymal cells (supplementary material Tables S1–S4) and that Igf2 stands out among the up-regulated genes (supplementary material Table S3). Of note, *Igf2* expression is quite high (~200-folds of that in ATDC5 cells) in the right forelimb tissue of E12.5 control mice, while it is reduced to ~70% in the mutant samples (Fig. 6C). The gene for Igf2 receptor, *Igf1r*, is expressed in both mesenchymal (ATDC5) and epithelial (MKE) cell lines, but the genes for its ligands (*Igf1* and *Igf2*) are expressed only in the mesenchymal cell line (data not shown). Enhancement of Igf2 expression by Reck, probably in the mesenchyme, should have a major impact on the growth and survival of both epithelial and mesenchymal cells in developing limbs, although the exact extent of the contribution of Igf2 to the present phenomenon remains to be tested in future studies. Reck also modifies the expression of several components involved in cytokine signaling (supplementary material Tables S3 and S4); possible contributions of these molecules to the health of limb tissues also need to be tested. The exact mechanism by which Reck, a GPI-anchored protein devoid of a cytoplasmic domain, affects gene expression remains presently unclear; a plausible mechanism is that Reck interferes with the cleavage or interaction of cell surface or peri-cellular proteins involved in intracellular signaling that impinge on gene expression.

Igf2, WNT7A, and Fgf8 upregulate Reck in ATDC5 cells (Fig. 6C), suggesting the presence of three positive feedback loops (i.e., reciprocal activation and/or maintenance) in the limb bud system: [1] a loop within the anterior mesenchyme (AM) mediated by Reck and Igf2, [2] a loop between the AM and DE mediated by Reck and Wnt7a, and [3] a loop between the AM and AER mediated by Reck and Fgfs (probably with Wnt7a) (Fig. 7C).

What do we learn from the other limb phenotypes? The round porous fingertips in the *Reck*-hypomorphic mice resemble several human conditions, including clubbed fingers, acro-osteolysis, and osteoporosis. These symptoms, however, have been correlated with diverse causes, and therefore the symptomatic resemblance is not very informative in elucidating its molecular basis. On the other hand, cutaneous horn is known as a rare precancerous skin tumor that may occur in various parts of the human body. Its exclusive occurrence on the dorsal side of extremities in *Reck*-hypomorphic mice may be another indication that reduced Reck impacts the limb bud DE. The precancerous nature of this phenotype is consistent with the activity of *Reck* to down-regulate several genes involved in "Pathways in Cancer" (Fig. 6A; supplementary material Table S2). It is unclear, however, why cutaneous horns occur in all extremities in the mutant mice while the postaxial bone defects occur exclusively in the forelimbs in a right-dominant fashion. This may reflect differences in the lineages and/or stages of target cells (e.g., keratinocytes vs. early limb bud mesenchyme/ectoderm) or in the levels of Reck required for the events (i.e., the cutaneous horns may arise with smaller decrease in Reck expression than the postaxial bone defects). It will be interesting to see whether RECK is down-regulated in human cutaneous horns and whether there is any correlation between the level of RECK and severity of the lesion. Further studies on the mechanism of cutaneous horn formation in the mutant mice may provide additional insights into how Reck works.

The reasons why the skeletal phenotype occurs only in the forelimbs in a right-dominant fashion in the low-*Reck* mice (Fig. 1H) is presently unclear. The observed difference in the levels of Reck expression among the four limbs (supplementary material Fig. S4) may provide a feasible explanation, although, other models such as temporal or spatial difference in the expression of functionally compensating genes, cannot be ruled out. Interestingly, *Wnt7a*-deficient mice show a similar, but milder, asymmetry in skeletal phenotype among the four limbs (Parr and McMahon, 1994), further supporting the relevance of Wnt7a-signaling to Reck's action in this system. Besides being a system useful in exploring several aspects of signal transduction and tissue interactions, the low-*Reck* mutant may also be useful in studying some fundamental issues in developmental biology such as forelimb-hindlimb dichotomy and lateral symmetry.

A variety of teratogens, including cadmium, acetazolamide, and ethanol, are known to induce a common limb malformation in mice after treatment at E9.5 (Bell et al., 2005; Schreiner et al., 2009). This malformation (postaxial, right-dominant forelimb ectrodactyly) is almost a perfect phenocopy of R_{Low}/- mice. Furthermore, some of these teratogens (e.g., cadmium, ethanol) were found to down-regulate Reck in ATDC5 cells (Fig. 6E), implicating Reck as a target of these agents in teratogenesis. Other teratogens which cause this phenotype such as acetazolamide and thalidomide, however, did not affect Reck expression, suggesting that they may target at some points down-stream of Reck or may damage limb DE via a different mechanism(s). Artificial Reck expression in mice in conjunction with teratogen-treatment may be useful in testing these possibilities.

In conclusion, this study has revealed the importance of mesenchymal Reck in the maintenance/expansion of three signaling centers (DE, AER, and ZPA) essential for mammalian limb patterning and has shed some fresh light on the molecular and cellular interactions underlying limb development and patterning (Fig. 7). The newly emerging role of Reck in supporting tissue interactions has broad implications in understanding its roles in other processes in embryogenesis as well as in tumorigenesis.

Acknowledgements

We are grateful to Dr. Shin-ichi Aizawa for advice in generating mutant mice, Dr. Philippe M. Soriano for R26R mouse, Dr. Andrew P. McMahon and Dr. Matthew Scott for WISH probes, and Dr. Maja Adamska for technical advice. We also thank Aiko Nishimoto, Hai-Ou Gu, and Mari Kojima for technical assistance, Aki Miyazaki for secretarial assistance, and all members of the laboratories for their help and advice. This work was supported by JSPS Grant-in-Aid for

Creative Scientific Research, MEXT Grant-in-Aid on Priority Areas, and MEXT Grant-in-Aid for Scientific Research on Innovative Areas.

Competing interests

The authors declare no competing financial interests.

References

Adamska, M., MacDonald, B. T., Sarmast, Z. H., Oliver, E. R. and Meisler, M. H. (2004). En1 and Wnt7a interact with Dkk1 during limb development in the mouse. *Dev. Biol.* **272**, 134-144.

Adamska, M., Billi, A. C., Cheek, S. and Meisler, M. H. (2005). Genetic interaction between Wnt7a and Lrp6 during patterning of dorsal and posterior structures of the mouse limb. *Dev. Dyn.* **233**, 368-372.

Ahn, S. and Joyner, A. L. (2004). Dynamic changes in the response of cells to positive hedgehog signaling during mouse limb patterning. *Cell* **118**, 505-516.

Akiyama, H., Chaboissier, M. C., Martin, J. F., Schedl, A. and de Crombrugghe, B. (2002). The transcription factor Sox9 has essential roles in successive steps of the chondrocyte differentiation pathway and is required for expression of Sox5 and Sox6. *Genes Dev.* **16**, 2813-2828.

Atsumi, T., Ikawa, Y., Miwa, Y. and Kimata, K. (1990). A chondrogenic cell line derived from a differentiating culture of AT805 teratocarcinoma cells. *Cell Differ. Dev.* **30**, 109-116.

Bell, S. M., Schreiner, C. M., Goetz, J. A., Robbins, D. J. and Scott, W. J., Jr. (2005). Shh signaling in limb bud ectoderm: potential role in teratogen-induced postaxial ectrodactyly. *Dev. Dyn.* **233**, 313-325.

Chandana, E. P., Maeda, Y., Ueda, A., Kiyonari, H., Oshima, N., Yamamoto, M., Kondo, S., Oh, J., Takahashi, R., Yoshida, Y. et al. (2010). Involvement of the Reck tumor suppressor protein in maternal and embryonic vascular remodeling in mice. *BMC Dev. Biol.* **10**, 84.

Chen, H., Lun, Y., Ovchinnikov, D., Kokubo, H., Oberg, K. C., Pepicelli, C. V., Can, L., Lee, B. and Johnson, R. L. (1998). Limb and kidney defects in Lmx1b mutant mice suggest an involvement of LMX1B in human nail patella syndrome. *Nat. Genet.* **19**, 51-55.

Chiang, C., Litingtung, Y., Lee, E., Young, K. E., Corden, J. L., Westphal, H. and Beachy, P. A. (1996). Cyclopia and defective axial patterning in mice lacking Sonic hedgehog gene function. *Nature* **383**, 407-413.

Chiang, C., Litingtung, Y., Harris, M. P., Simandl, B. K., Li, Y., Beachy, P. A. and Fallon, J. F. (2001). Manifestation of the limb prepattern: limb development in the absence of sonic hedgehog function. *Dev. Biol.* **236**, 421-435.

Collette, N. M., Genetos, D. C., Murugesh, D., Harland, R. M. and Loots, G. G. (2010). Genetic evidence that SOST inhibits WNT signaling in the limb. *Dev. Biol.* **342**, 169-179.

Conlon, R. A. and Rossant, J. (1992). Exogenous retinoic acid rapidly induces anterior ectopic expression of murine Hox-2 genes in vivo. *Development* **116**, 357-368.

DeChiara, T. M., Efstratiadis, A. and Robertsen, E. J. (1990). A growth-deficiency phenotype in heterozygous mice carrying an insulin-like growth factor II gene disrupted by targeting. *Nature* **345**, 78-80.

Gomi, H., Yokoyama, T., Fujimoto, K., Ikeda, T., Katoh, A., Itoh, T. and Itohara, S. (1995). Mice devoid of the glial fibrillary acidic protein develop normally and are susceptible to scrapie prions. *Neuron* **14**, 29-41.

Hatta, M., Matsuzaki, T., Morioka, Y., Yoshida, Y. and Noda, M. (2009). Density- and serum-dependent regulation of the Reck tumor suppressor in mouse embryo fibroblasts. *Cell. Signal.* **21**, 1885-1893.

Johnson, R. L. and Tabin, C. J. (1997). Molecular models for vertebrate limb development. *Cell* **90**, 979-990.

Kondo, S., Shukunami, C., Morioka, Y., Matsumoto, N., Takahashi, R., Oh, J., Atsumi, T., Umezawa, A., Kudo, A., Kitayama, H. et al. (2007). Dual effects of the membrane-anchored MMP regulator RECK on chondrogenic differentiation of ATDC5 cells. *J. Cell Sci.* **120**, 849-857.

Kraus, P., Fraidenraich, D. and Loomis, C. A. (2001). Some distal limb structures develop in mice lacking Sonic hedgehog signaling. *Mech. Dev.* **100**, 45-58.

Lakso, M., Pichel, J. G., Gorman, J. R., Sauer, B., Okamoto, Y., Lee, E., Alt, F. W. and Westphal, H. (1996). Efficient in vivo manipulation of mouse genomic sequences at the zygote stage. *Proc. Natl. Acad. Sci. USA* **93**, 5860-5865.

Logan, M., Martin, J. F., Nagy, A., Lobe, C., Olson, E. N. and Tabin, C. J. (2002). Expression of Cre Recombinase in the developing mouse limb bud driven by a Prxl enhancer. *Genesis* **33**, 77-80.

Mariani, F. V., Ahn, C. P. and Martin, G. R. (2008). Genetic evidence that FGFs have an instructive role in limb proximal-distal patterning. *Nature* **453**, 401-405.

McGlinn, E. and Tabin, C. J. (2006). Mechanistic insight into how Shh patterns the vertebrate limb. *Curr. Opin. Genet. Dev.* **16**, 426-432.

McLeod, M. J. (1980). Differential staining of cartilage and bone in whole mouse fetuses by alcian blue and alizarin red S. *Teratology* **22**, 299-301.

Michos, O., Panman, L., Vintersten, K., Beier, K., Zeller, R. and Zuniga, A. (2004). Gremlin-mediated BMP antagonism induces the epithelial-mesenchymal feedback signaling controlling metanephric kidney and limb organogenesis. *Development* **131**, 3401-3410.

Miki, T., Takegami, Y., Okawa, K., Muraguchi, T., Noda, M. and Takahashi, C. (2007). The reversion-inducing cysteine-rich protein with Kazal motifs (RECK) interacts with membrane type 1 matrix metalloproteinase and CD13/aminopeptidase N and modulates their endocytic pathways. *J. Biol. Chem.* **282**, 12341-12352.

Morioka, Y., Monypenny, J., Matsuzaki, T., Shi, S., Alexander, D. B., Kitayama, H. and Noda, M. (2009). The membrane-anchored metalloproteinase regulator RECK stabilizes focal adhesions and anterior-posterior polarity in fibroblasts. *Oncogene* **28**, 1454-1464.

Muraguchi, T., Takegami, Y., Ohtsuka, T., Kitajima, S., Chandana, E. P., Omura, A., Miki, T., Takahashi, R., Matsumoto, N., Ludwig, A. et al. (2007). RECK modulates Notch signaling during cortical neurogenesis by regulating ADAM10 activity. *Nat. Neurosci.* **10**, 838-845.

Niswander, L. (2003). Pattern formation: old models out on a limb. *Nat. Rev. Genet.* **4**, 133-143.

Noda, M. and Takahashi, C. (2007). Recklessness as a hallmark of aggressive cancer. *Cancer Sci.* **98**, 1659-1665.

Oh, J., Takahashi, R., Kondo, S., Mizoguchi, A., Adachi, E., Sasahara, R. M., Nishimura, S., Imamura, Y., Kitayama, H., Alexander, D. B. et al. (2001). The membrane-anchored MMP inhibitor RECK is a key regulator of extracellular matrix integrity and angiogenesis. *Cell* **107**, 789-800.

Omura, A., Matsuzaki, T., Mio, K., Ogura, T., Yamamoto, M., Fujita, A., Okawa, K., Kitayama, H., Takahashi, C., Sato, C. et al. (2009). RECK forms cowbell-shaped dimers and inhibits matrix metalloproteinase-catalyzed cleavage of fibronectin. *J. Biol. Chem.* **284**, 3461-3469.

Ovchinnikov, D. A., Deng, J. M., Ogunrinu, G. and Behringer, R. R. (2000). Col2a1-directed expression of Cre recombinase in differentiating chondrocytes in transgenic mice. *Genesis* **26**, 145-146.

Parr, B. A. and McMahon, A. P. (1994). Dorsalizing signal Wnt-7a required for normal polarity of D-V and A-P axes of mouse limb. *Nature* **374**, 350-353.

Prifti, E., Zucker, J. D., Clement, K. and Henegar, C. (2008). FunNet: an integrative tool for exploring transcriptional interactions. *Bioinformatics* **24**, 2636-2638.

Riddle, R. D., Ensini, M., Nelson, C., Tsuchida, T., Jessell, T. M. and Tabin, C. (1995). Induction of the LIM homeobox gene Lmx1 by WNT7a establishes dorsoventral pattern in the vertebrate limb. *Cell* **83**, 631-640.

Sasahara, R. M., Takahashi, C., Sogayar, M. C. and Noda, M. (1999). Oncogene-mediated downregulation of RECK, a novel transformation suppressor gene. *Braz. J. Med. Biol. Res.* **32**, 891-895.

Saunders, J. W., Jr. (1948). The proximo-distal sequence of origin of the parts of the chick wing and the role of the ectoderm. *J. Exp. Zool.* **108**, 363-403.

Schreiner, C. M., Bell, S. M. and Scott, W. J., Jr. (2009). Microarray analysis of murine limb bud ectoderm and mesoderm after exposure to cadmium or acetazolamide. *Birth Defects Res. A Clin. Mol. Teratol.* **85**, 588-598.

Selever, J., Liu, W., Lu, M. F., Behringer, R. R. and Martin, J. F. (2004). Bmp4 in limb bud mesoderm regulates digit pattern by controlling AER development. *Dev. Biol.* **276**, 268-279.

Shukunami, C., Shigeno, C., Atsumi, T., Ishizeki, K., Suzuki, F. and Hiraki, Y. (1996). Chondrogenic differentiation of clonal mouse embryonic cell line ATDC5 in vitro: differentiation-dependent gene expression of parathyroid hormone (PTH)/PTH-related peptide receptor. *J. Cell Biol.* **133**, 457-468.

Smith, S. M. and Cartwright, M. M. (1997). Spatial visualization of apoptosis using a whole-mount in situ DNA end-labeling technique. *Biotechniques* **22**, 832-834.

Soriano, P. (1999). Generalized lacZ expression with the ROSA26 Cre reporter strain. *Nat. Genet.* **21**, 70-71.

Sun, X., Mariani, F. V. and Martin, G. R. (2002). Functions of FGF signalling from the apical ectodermal ridge in limb development. *Nature* **418**, 501-508.

Tabin, C. and Wolpert, L. (2007). Rethinking the proximodistal axis of the vertebrate limb in the molecular era. *Genes Dev.* **21**, 1433-1442.

Takahashi, C., Sheng, Z., Horan, T. P., Kitayama, H., Maki, M., Hitomi, K., Kitaura, Y., Takai, S., Sasahara, R. M., Horimoto, A. et al. (1998). Regulation of matrix metalloproteinase-9 and inhibition of tumor invasion by the membrane-anchored glycoprotein RECK. *Proc. Natl. Acad. Sci. USA* **95**, 13221-13226.

Taniguchi, M., Yuasa, S., Fujisawa, H., Naruse, I., Saga, S., Mishina, M. and Yagi, T. (1997). Disruption of *semaphorin III/D* gene causes severe abnormality in peripheral nerve projection. *Neuron* **19**, 519-530.

Tickle, C. (2006). Making digit patterns in the vertebrate limb. *Nat. Rev. Mol. Cell Biol.* **7**, 45-53.

Towers, M. and Tickle, C. (2009). Growing models of vertebrate limb development. *Development* **136**, 179-190.

Wurst, W., Auerbach, A. B. and Joyner, A. L. (1994). Multiple developmental defects in Engrailed-1 mutant mice: an early mid-hindbrain deletion and patterning defects in forelimbs and sternum. *Development* **120**, 2065-2075.

Yang, Y. and Niswander, L. (1995). Interaction between the signaling molecules WNT7a and SHH during vertebrate limb development: dorsal signals regulate anteroposterior patterning. *Cell* **80**, 939-947.

Zeller, R., López-Ríos, J. and Zuniga, A. (2009). Vertebrate limb bud development: moving towards integrative analysis of organogenesis. *Nat. Rev. Genet.* **10**, 845-858.

Zhu, J., Nakamura, E., Nguyen, M. T., Bao, X., Akiyama, H. and Mackem, S. (2008). Uncoupling Sonic hedgehog control of pattern and expansion of the developing limb bud. *Dev. Cell* **14**, 624-632.